LIGHT CURVES OF RETIRED GEOSYNCHRONOUS SATELLITES

C. Benson[(1)], D. J. Scheeres[(1)], and N. Moskovitz[(2)]

[(1)]*University of Colorado at Boulder, Boulder, CO, 80309, USA, Email: {conor.j.benson, scheeres}@colorado.edu*
[(2)]*Lowell Observatory, Flagstaff, AZ, 86001, USA, Email: nmosko@lowell.edu*

ABSTRACT

Photometric light curve observations of several retired geosynchronous satellites are presented. These data were collected at Lowell Observatory in Flagstaff, Arizona during July 2016. Preliminary analysis of the light curves is conducted using Fourier series, Fourier transform, and phase folding methods to determine plausible rotation states. Satellites were found to have a variety of rotation states ranging from uniform to complex tumbling motion. For previously observed satellites, the potential for rotation state evolution is discussed. Analysis shows that two nearly identical weather satellites, GOES 8 and GOES 9, appear to be evolving quite differently. GOES 8 has progressed from uniform to increasingly complex tumbling motion since 2014 whereas the tumbling state of GOES 9 does not appear to have changed during this same span. Better understanding of the rotation state evolution of these retired geosynchronous satellites and others promises to improve estimates for attitude dependent solar radiation pressure forces, help assess potential for material shedding, and aid in on-orbit debris mitigation and recycling efforts.

Key words: retired geosynchronous satellites, light curves, rotation states.

1. INTRODUCTION

With the growing value of the geosynchronous ring for communications and observation, understanding the debris in this region is all the more important. The geosynchronous region is especially susceptible to space debris accumulation given the absence of atmospheric drag. Without this natural de-orbiting process, objects will remain in orbit indefinitely. There are currently more than 700 known debris objects in the geosynchronous region [6]. Debris objects of particular interest are retired and otherwise inactive satellites in or near geosynchronous Earth orbit (GEO). While the orbital dynamics of these satellites have been extensively studied, little is understood about their rotational motion. However, many are known to spin rapidly or have evolving rotation states [4, 9, 11, 14]. In 2015 alone, at least 13 satellites in or near GEO were retired, 7 of which were not re-orbited in accordance with IADC guidelines [6]. With both the value and debris population of the GEO region increasing, it is worthwhile to investigate retired satellite rotation states.

Better knowledge of this rotation state evolution stands to improve long term orbit predictions through more accurate modeling of attitude dependent solar radiation pressure forces. In addition, this knowledge will help assess the potential for material shedding in satellites with fast spin rates. Finally, it will aid in on-orbit debris mitigation and recycling efforts where rotation state estimates are invaluable for successfully grappling non-cooperative and potentially tumbling or rapidly spinning satellites.

At end of life, GEO satellites are generally boosted above the main ring and decommissioned, where they drift westward at 4-5 degrees per day. This slow motion means particular satellites are visible for several weeks at a time and return to view every 2-3 months. Given their slow relative motion, retired GEO satellites are prime targets for ground-based optical observation. Furthermore, their periodic viewing opportunities allow for the evolving rotational motion to be studied.

One particularly notable group of retired satellites are NOAA's Loral-contracted second generation Geostationary Operational Environment Satellites (GOES), an example of which is shown in Figure 1. This group of five satellites, GOES 8 through 12, are nearly identical and were retired in order between 2004 and 2013. Extensive photometric observations of these satellites have been gathered over the past several years by Cognion and Ryan and Ryan [4, 14]. These authors showed that GOES 8 was in uniform rotation with a period that increased from 16.83 s to 75.66 s between December 2013 and July 2014. Similarly, Cognion found that the rotation period of GOES 10 varied from 31.1 to 26.2 s between February and August 2014. Cognion also observed GOES 9, 11, and 12. These three satellites were in slow, tumbling motion with best-fit phase folded rotation periods ranging from 9 to 23 minutes.

In 2015, Albuja et al. hypothesized that the observed rotation state evolution of these and other retired GEO satellites is largely due to the Yarkovksy-O'Keefe-Radzievskii-Paddack (YORP) effect, a phenomenon in

Proc. 7th European Conference on Space Debris, Darmstadt, Germany, 18–21 April 2017, published by the ESA Space Debris Office
Ed. T. Flohrer & F. Schmitz, (http://spacedebris2017.sdo.esoc.esa.int, June 2017)

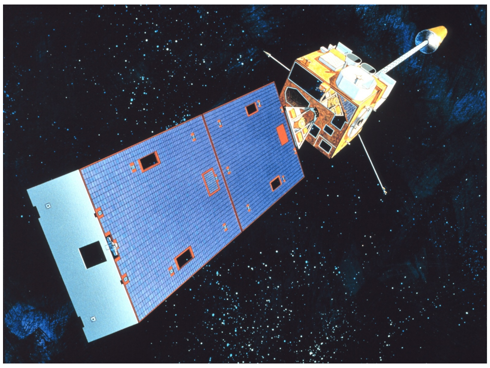

Figure 1. Illustration of 2nd Generation NOAA GOES Satellite [12]

which solar radiation absorption, reflection, and re-emission causes torques on an orbiting body [1]. More recently, Albuja et al. showed that the evolution predicted by YORP theory was consistent with observed GOES 8 and 10 uniform rotation periods [2]. Furthermore, Albuja et al. hypothesized that given its observed deceleration, GOES 8 would soon begin to tumble. Observations of GOES 8 gathered in September 2015 and February 2016 by Ryan and Ryan appear to confirm this [2, 14]. In light of these findings, Albuja et al. have suggested that the observed rotation state evolution of GOES 8 and 10 are part of a larger cyclical process. They hypothesize that due to the combined influence of YORP, energy dissipation, and other environmental factors, a satellite will spin up and down over time in addition to experiencing alternating periods of uniform and tumbling motion [2].

To explore this cyclical evolution hypothesis and better understand the rotational behavior, we have gathered additional photometric observations of GOES satellites and other retired GEO satellites. In the following sections, we will present these new light curve observations as well as preliminary analysis of the rotation periods. For the GOES satellites, observations are compared with those of Cognion and Ryan and Ryan to determine the potential for rotation state evolution.

2. METHODOLOGY

The following photometric observations were gathered using Lowell Observatory's 42 inch Hall and 72 inch Perkins telescopes in July 2016. These telescopes are both located at the observatory's Anderson Mesa facility south of Flagstaff, Arizona. The 42 inch Hall is an f/8 Ritchey-Chretien Cassegrain telescope with 1.04 m primary mirror and an EV2 CCD231 4096$\times$4112 pixel CCD. This configuration yields an unbinned pixel scale of 0.327 arcseconds per pixel. A VR filter was used for the Hall observations. The 72 inch Perkins is an f/17.5 Cassegrain telescope with a 1.8 m primary mirror and a 2048$\times$2064 pixel CCD yielding an unbinned pixel scale of 0.39 arcseconds per pixel. All Perkins observations were gathered with an R filter. For both telescopes, 3x3 pixel binning and 1 s exposure times were used. These configurations yielded sampling cadences of 11 s and 7 s for the Hall and Perkins telescopes respectively. For both telescopes, the observation time stamps are at the middle of the exposure. It should also be noted that all observations were taken at elevations greater than 30 degrees.

For pointing, two line elements sets were used to propagate each satellite's state forward in time using the Systems Tool Kit (STK) commercial software package. Both telescopes are fixed on equatorial mounts so these states were converted to astrometric right ascension, declination, and corresponding rates as pointing coordinates. To initialize tracking of a target, the telescope was slewed to the desired right ascension and declination at a future epoch. At the epoch, the corresponding right ascension and declination rates were initiated and the telescope began slewing at these constant rates. Images of the target were then taken until the target's time-varying rates caused it to begin drifting out of the field of view. At this point, tracking was paused while the pointing and rates were re-initialized at a future point, after which tracking and image capture was resumed. This approach was required due to each telescope's lack of an automated target pointing system. These telescopes are primarily used for observing asteroids and stars where only sidereal tracking is required. Depending on the rotation periods from previous observations and the observed frame to frame magnitude variation, targets were tracked for 15 minutes to an hour.

The images were reduced using the Image Reduction and Analysis Facility (IRAF) software suite and a custom IDL pipeline. For the 42 inch Hall images, star streaks were matched to the 2MASS star catalog to calibrate the satellite magnitudes and remove atmospheric extinction effects. The 72 inch Perkins images were reduced to yield instrument magnitudes only. It is suspected that small vibrations in Perkins the pointing system given the relatively large non-sidereal slew rates caused the star streaks to appear as having two or more centroids. This prevented the pipeline from successfully matching star streaks to catalog stars. Fortunately, given the clear conditions on the observing nights, this did not affect the reduced magnitudes significantly. Also, any data points with clear field star contamination were flagged and removed.

3. LIGHT CURVES AND ANALYSIS

3.1. GOES 8

The first satellite to discuss is GOES 8. This satellite was observed using Lowell's 72 inch Perkins telescope on July 14, 2016. The resulting light curve is shown in the bottom plot of Figure 2. Previous GOES 8 light curves taken at Magdalena Ridge Observatory (MRO) in New Mexico are also shown in Figure 2 for comparison courtesy of William and Eileen Ryan [2, 14]. On initial inspection, all three light curves appear to deviate from periodic structure. While the sun-satellite-earth phase angles changed during each observation span, the differences between the initial and final angles were 29° - 26°, 23° - 34°, and 70° - 66° respectively. These changes of 3° to 11° are not likely to introduce the observed aperiodic structure to a uniformly rotating body's light curve. This indicates that the lack of clear periodicity is due instead to tumbling motion at all three epochs. Another trend over these three light curves is that the structure and periodicity becomes less defined over time, suggesting temporal evolution of the satellite's rotation state. For the September 2015 light curve, the smaller peaks are spaced approximately 8 minutes apart. The February 2016 light curve has similar structure, but now with a semi period of approximately 12 minutes strongly suggesting rotation state evolution. By July 2016, the light curve structure appears quite complex, with no clear periodicity. It should be noted that any observed periods are the synodic periods rather than the satellite's inertial (sidereal) rotation periods. Hall et al. show that these two periods are related through the phase angle bisector [7].

An interesting observation from the most recent light curve is the trend towards increasing magnitude over time. Given the small change in phase angle during this observation span, 70° - 66°, this roughly two magnitude change in brightness is not likely due to phase angle variation. By observing numerous controlled geosynchronous satellites at varying phase angles, Cognion found that the brightness generally varied by only 0.2 magnitudes for a phase angle change of 66° to 70° [3]. While atmospheric variations can also affect the mean magnitude, a five fold reduction in brightness would require significant cloud cover. Yet, Lowell Observatory's all sky camera showed clear skies during this observation span. So, the observed magnitude increase is likely dominated by the satellite's rotation alone.

Given the light curve's sparsity and the strong dependence of light curve structure on viewing geometry, it is not immediately clear whether the observed differences in the July 2016 light curve are due to rotation state evolution or different viewing geometry [15]. To determine which it is, we will conduct a preliminary analysis of the February and July 2016 light curves tumbling periods. A fundamental assumption in the following analysis is that the body is in torque-free motion during the observation span. For large geosynchronous satellites, rotational evolution takes orders of magnitude longer than any practical observation span. This ultimately means that the sidereal rotation periods can be taken as constant for the entire light curve. Unlike with uniform rotation, torque-free tumbling motion has two fundamental periods. The first period corresponds to rotation of the body about either extremal principal axis (axis of minimum or maximum inertia). The second period corresponds to precession of this extremal principal axis about the rotational angular momentum vector [8]. Furthermore, given a particular period convention, a tumbling rotation state has only one possible pair of periods [15]. So light curves with different fundamental periods have different tumbling rotation

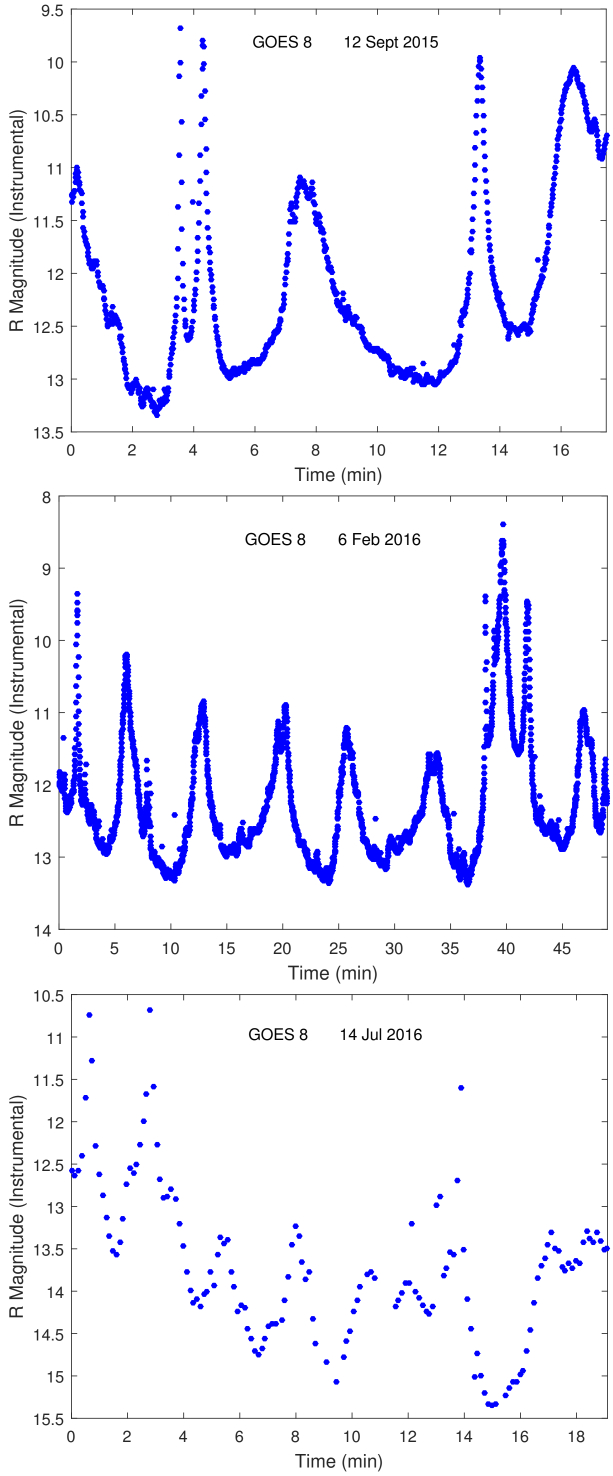

Figure 2. GOES 8 light curves - Top: Sept. 12, 2015 (MRO 2.4 m) Middle: Feb. 6, 2016 (MRO 2.4 m) Bottom: Jul. 14, 2016 (Lowell 72 in)

states. These two periods are generally incommensurate, yielding motion where the body never returns to the same orientation in a fixed interval [15]. This translates to a lack of periodicity in tumbling light curves.

In asteroid research, the fundamental tumbling periods are often analyzed by fitting a two-dimensional Fourier series [8, 13] to the light curve. When expressed as a two-dimensional Fourier series, the light curve magnitude $B(t)$ is given by,

$$\begin{aligned} B(t) &= C_0 + \sum_{i=1}^{m} \Big[C_{i0} \cos i\omega_1 t + S_{i0} \sin i\omega_1 t \Big] \\ &+ \sum_{j=1}^{m} \sum_{i=-m}^{m} \Big[C_{ij} \cos{(i\omega_1 + j\omega_2)t} \\ &+ S_{ij} \sin{(i\omega_1 + j\omega_2)t} \Big] \end{aligned} \quad (1)$$

where m is the Fourier series order, C_0 is the mean light curve brightness, C_{ij} and S_{ij} are the Fourier series coefficients for frequency harmonic (i,j), and the two fundamental frequencies are given by $\omega_1 = \frac{2\pi}{P_1} = 2\pi f_1$ and $\omega_2 = \frac{2\pi}{P_2} = 2\pi f_2$ where P_1 and P_2 are the fundamental periods. It should be noted that the two-dimensional Fourier Series provides no information about which of the two periods correspond to rotation and precession, only whether the pair fits the light curve well.

In practice, one searches a variety of period pairs, fitting each to the light curve with a least squares Fourier series fit. The goal is then to find the period pair that minimizes the root-mean-square (RMS) error between the observations and modeled light curve. This is given by,

$$RMS = \sqrt{\frac{1}{n}\sum_{i=1}^{n}(O_i - B_i)^2} \quad (2)$$

where n is the number of observations and O_i and B_i are the observed and modeled brightness at the ith observation time.

For both 2016 GOES 8 light curves, periods from 30 s to 30 min were surveyed using a 2nd order ($m = 2$) Fourier series. A 2nd order fit was used because the most dominant light curve frequencies are often no higher than the 2nd harmonic [8, 13, 15]. This allows one to fit to the major light curve features while keeping the free parameters to a minimum. The results are provided in Figures 3 and 4. For each figure, only half of the domain is shown because there is no distinction between P_1 and P_2 in the Fourier series (i.e. the fits will be mirrored along the $P_1 = P_2$ line). The period pairs with the best fits show up in dark blue. We can see that the well-fitting periods are very different for the two light curves. For the February 2016 light curve, the best-fitting pair is P_1 = 14.52 min and P_2 = 12.27 min. For July 2016, many periods of approximately 4 minutes fit well. This dispersion of well-fitting solutions may be due to the sparsity of the light curve. Nevertheless, the best fit occurs for P_1 = 20.65 min and P_2 = 3.95 min.

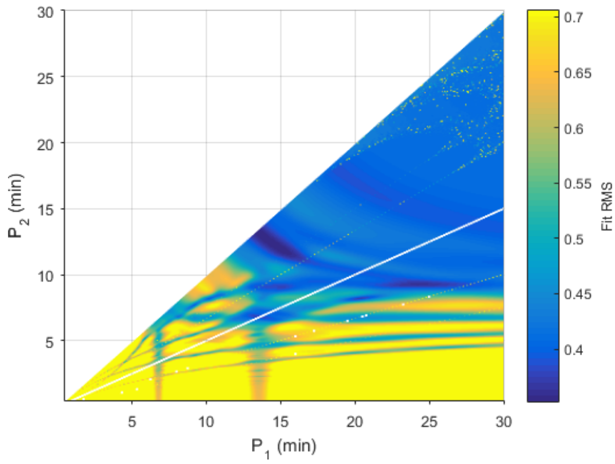

Figure 3. 2nd order ($m = 2$) 2-D Fourier Series RMS values for Feb. 6, 2016 GOES 8 light curve.

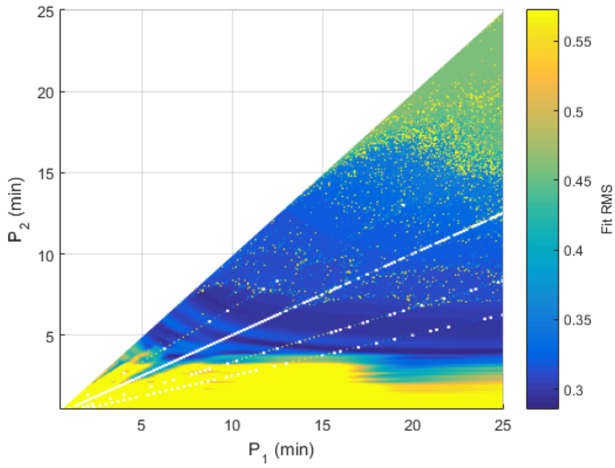

Figure 4. 2nd order ($m = 2$) 2-D Fourier Series RMS values for Jul. 14, 2016 GOES 8 light curve.

The 2nd order fits for these period pairs are shown in Figures 5 and 6. We can see that to 2nd order, both fits closely match the major features apart from the short, bright glints. This is to be expected as higher order harmonics would be needed to fit these higher frequency features. Overall, the very different well-fitting fundamental frequencies for the February and July 2016 GOES 8 light curves are a strong indication that the apparent changes in light curve structure are due to evolution of the satellite's tumbling rotation state rather than viewing geometry.

3.2. GOES 9

GOES 9 was observed on July 3, 2016 using Lowell Observatory's 42 inch Hall telescope. Observations were taken for an hour over an increasing phase angle of 9° to 21°. The reduced light curve is shown in Figure 7. Given the lack of clear periodicity, it is likely that the satellite is in tumbling motion. Cognion observed GOES 9 almost exactly two years earlier on July 4, 2014 and found a light

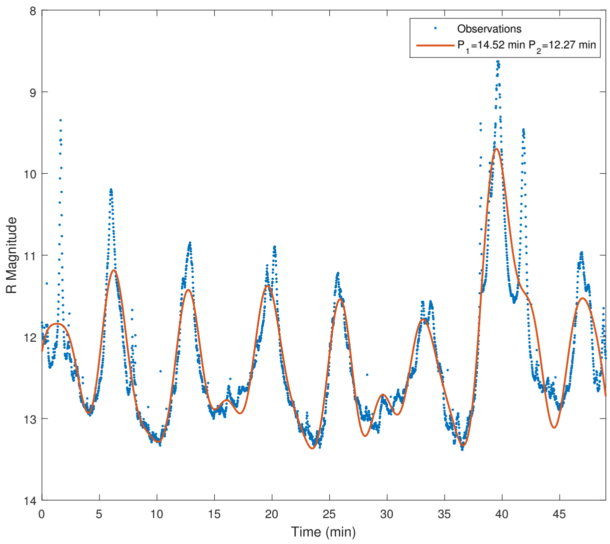

Figure 5. 2nd order ($m = 2$) 2-D Fourier Series fit for Feb. 6, 2016 GOES 8 light curve.

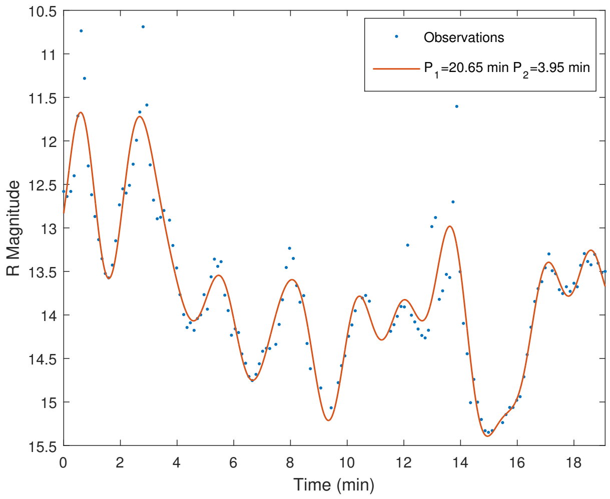

Figure 6. 2nd order ($m = 2$) 2-D Fourier Series fit for Jul. 14, 2016 GOES 8 light curve.

curve with very similar structure to that from 2016 [4]. In fact on closer inspection, the last 25 minutes of the 2014 light curve are nearly identical to the first 25 minutes of the 2016 light curve, with even the small single-image features being replicated. This strongly suggests that the satellite's rotation state did not change significantly over this two year span. Using single period phase folding, Cognion found that the best-fitting periods in 2014 were at 9.1 and 22.7 min [4]. Since the 2016 light curve covers a significant number of cycles, it is useful to convert into the frequency domain using a Fourier transform. When expressed in the frequency domain, the dominant light curve frequencies are exposed. For tumbling bodies, these frequencies are generally small integer linear combinations of the two fundamental frequencies [8]. Due to the gap in the GOES 9 light curve from 35 to 40 min, only the first 35 min were used to avoid spurious frequencies caused by non uniform sampling rates. Algorithms do exist for removing spurious frequencies due to non-uniform sampling and observation gaps [10]. The resulting Fourier transform is provided in Figure 8. Here we can see that there are several dominant frequencies. Starting from the left, the four largest peaks are at 0.0646, 0.162, 0.259, and 0.517 cycle/min.

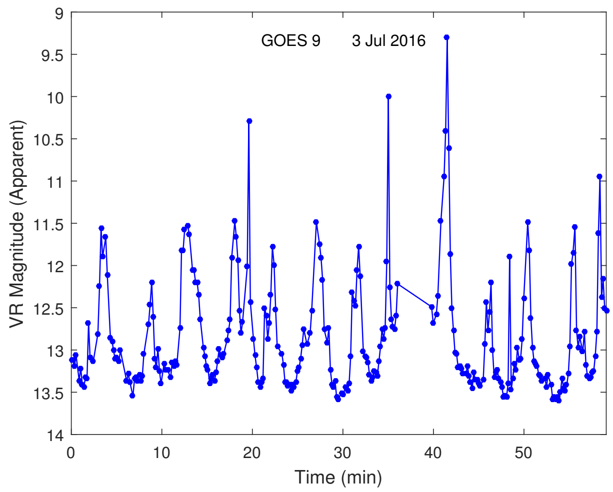

Figure 7. GOES 9 light curve Jul. 3, 2016 (Lowell 42 in)

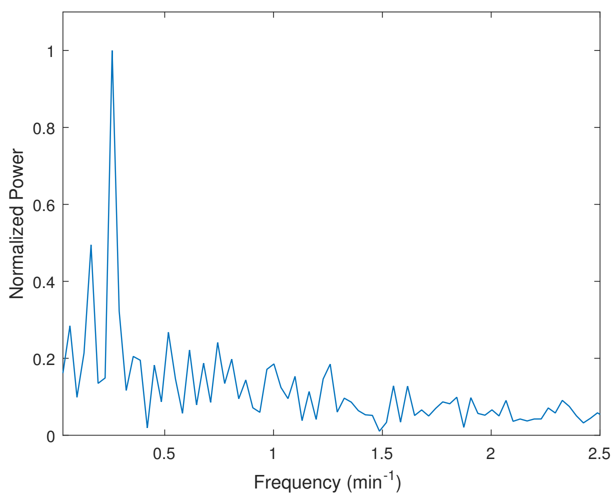

Figure 8. Fourier Transform of GOES 9 light curve

A tumbling period grid search can also be conducted. No period pairs fit the 2016 GOES 9 light curve well for a 2nd order 2-D Fourier series given the intricate features, but the best-fitting pair for 3rd and 4th order fits was P_1=15.14 min and P_2=5.74 min. The 4th order fit of these periods is provided in Figure 9. While the fit magnitude diverges in the observation gap due to a lack of data, the fit generally matches the major structure and periodicity well. Furthermore, linear combinations of the frequencies f_1 and f_2 corresponding to P_1 and P_2 yield frequencies similar to the Fourier transform peak frequencies: $f_1 = 0.0661$, $f_2 = 0.174$, $f_1 + f_2 = 0.24$, and $2f_1 + 2f_2 = 0.48$. The frequency $f_2 - f_1$ corresponds to a period of 9.25 min, similar to one of

Cognion's best-fitting phase folded periods for the 2014 light curve. These five low order linear combinations are often present in tumbling light curves [8, 13, 15]. Given these consistencies and the nearly identical structure of the two light curves, it appears that GOES 9 maintained the same rotation state between July 2014 and July 2016 with plausible rotation periods of P_1 = 15.14 min and P_2 = 5.74 min.

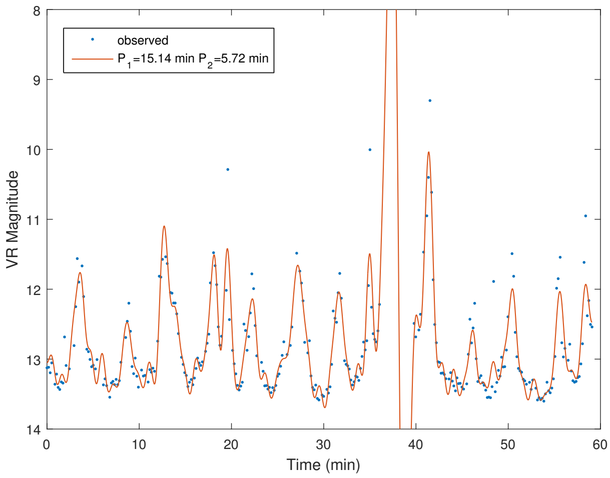

Figure 9. 4th order (m = 4) 2-D Fourier Series fit for Jul. 3, 2016 GOES 9 light curve.

3.3. GOES 10

GOES 10 was observed on July 14, 2016 using Lowell's 72 inch Perkins telescope over a phase angle range of 40° to 34°. The reduced light curve is shown in Figure 10. Cognion observed GOES 10 in uniform motion with rotation period that decreased from 31.1 s to 26.2 s between February and August 2014 [4]. Each of Cognion's three light curves show four distinct peaks in brightness per rotation period. One possible interpretation of the July 2016 light curve is uniform motion with three peaks followed by a dimming in brightness. If this is the case, the rotation period would be approximately 9 minutes, significantly longer than in 2014. Nevertheless, the rapid fluctuations in brightness between peaks and the peak non-uniformity suggest that the light curve may be under-sampled or that the satellite is in tumbling motion. Attempts to phase fold the light-curve to each of Cognion's rotation periods proved inconclusive. Structure was only found at multiples of the 7 s sampling rate. Given the 2016 light curve's sparse sampling and short duration, more observations are likely needed to determine a current rotation state for GOES 10.

3.4. Astra 1C

Astra 1C is geosynchronous satellite that was retired in 2014 [5]. It was observed on July 15, 2016 using Lowell's 72 inch Perkins telescope. The phase angle varied

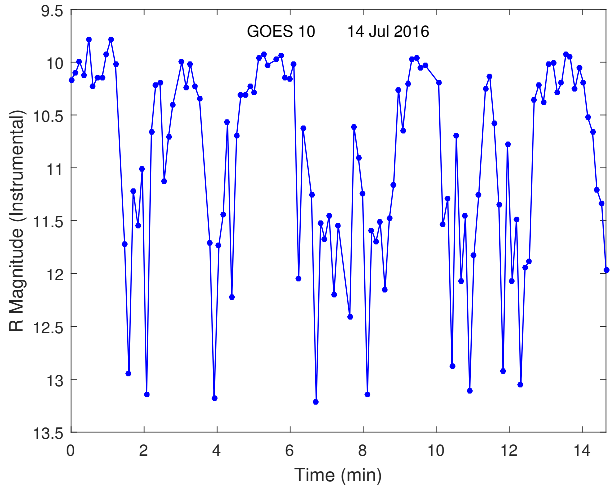

Figure 10. GOES 10 light curve Jul. 14, 2016 (Lowell 72 in)

from 31° to 27° over the 13 minute observation span. The reduced light curve for Astra 1C is shown in Figure 11. As with GOES 9, the telescope slew rates needed adjustment during the observation arc, resulting in a several minute gap in the light curve. The periodicity of the light curve is clearly visible with two opposing peaks per rotation period. The satellite appears to be in uniform or nearly uniform motion. The differences in peak structure are likely due to under-sampling. Nevertheless, there are sufficient rotation periods to phase fold the light curve and determine the rotation period. The phase folded light curve is shown in Figure 12. The period with the best fit was found to be 189.1 s with the uncertainty given by the range of periods with similar dispersion. Given that this satellite was recently retired and no other known observations exist, it will be interesting to see how its rotation state evolves with future observations.

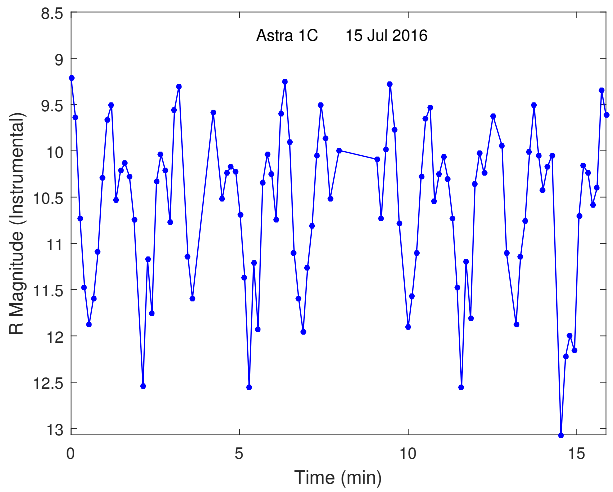

Figure 11. Astra 1C light curve Jul. 15, 2016 (Lowell 72 in)

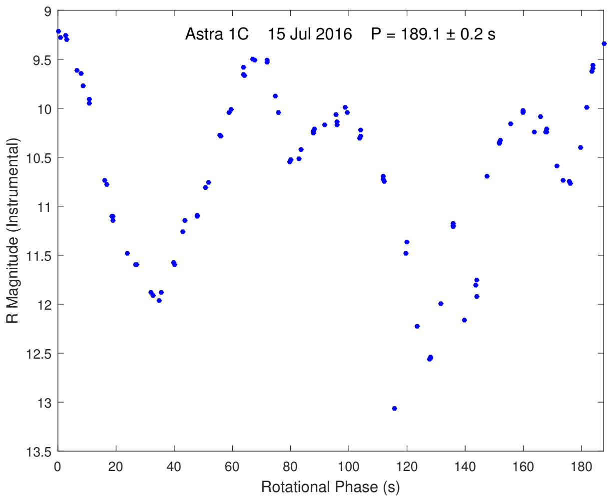

Figure 12. Phase Folded Astra 1C light curve

3.5. Inmarsat-2 F2

Inmarsat-2 F2 is a retired geosynchronous satellite that reached end of life in 2014 [5]. It was observed on July 15, 2016 with Lowell's 72 inch Perkins telescope over a decreasing phase angle of 33° to 26°. The reduced light curve is provided in Figure 13. The large, non-periodic fluctuations in magnitude suggest that the satellite is in a tumbling rotation state. Given that the phase angle change is relatively small and the light curve magnitudes are similar near the beginning and end of the light curve, the large magnitude fluctuations are not likely due to changing viewing geometry.

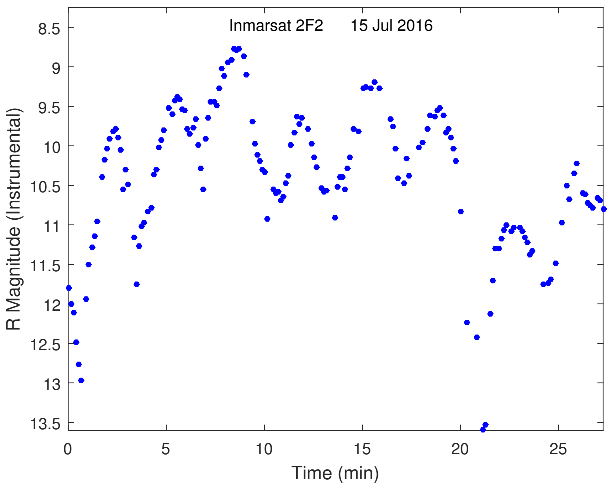

Figure 13. Inmarsat-2 F2 light curve Jul. 15, 2016 (Lowell 72 in)

To determine the best-fitting fundamental tumbling periods for the Inmarsat-2 F2 light curve, a period grid search was conducted for 2nd order. The best-fitting pair was found to be P_1 = 7.83 min and P_2 = 7.67 min. This light curve fit is provided in Figure 14. Since these periods are nearly equal, one would expect a single period to fit the light curve well, yet no single period Fourier series through 4th order yielded a plausible fit. This suggests that the satellite is tumbling. Inmarsat-2 F2 will be observed in the future to monitor any changes in its rotation state.

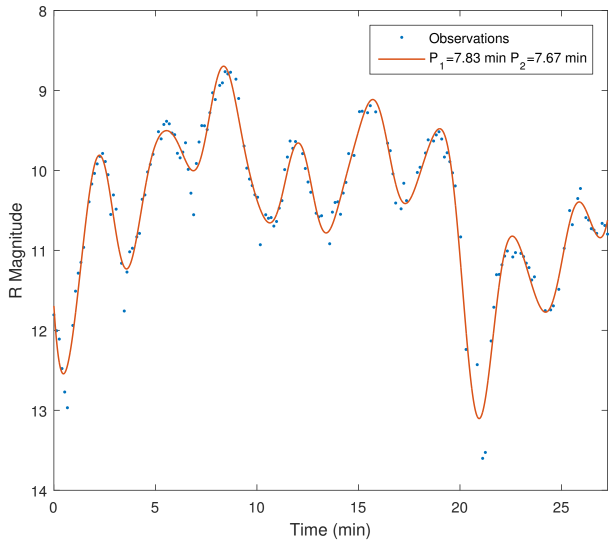

Figure 14. 2nd Order ($m = 2$) 2-D Fourier Series fit for Inmarsat-2 F2 light curve

4. DISCUSSION

An intrinsic goal of the July 2016 satellite observation campaign was to assess the viability of Lowell Observatory's 42 inch Hall and 72 inch Perkins optical telescopes for retired satellite observations. These two telescopes are primarily used to observe asteroids, comets, stars, and galaxies where only sidereal tracking is generally needed. Earth satellite observation places greater requirements on tracking and sampling rates. While both telescopes were able to successfully track the targets at the desired slew rates, the limitations of manual pointing were apparent. Without the ability to command time-varying slew rates, observations had to be paused periodically to re-point the telescopes, resulting in gaps in the light curves. Ultimately, these tracking limitations did not significantly affect the results, as clear conclusions were drawn from the GOES 9 and Astra 1C light curves. Nevertheless, implementing time-varying tracking rates for Lowell's telescopes will be explored for future observation campaigns. The bigger limitation with the current telescope configurations is the low sampling cadence. The sampling cadences were 11 s and 7 s for the Hall and Perkins telescopes respectively, limiting viable targets to those with slow spin rates. Even for many of the slowly spinning satellites, the light curves were under-sampled. A large fraction of this sampling time is spent reading out the CCD. Fortunately, there are several adjustments that can be made to significantly reduce the readout times. For these observations, the CCDs of both telescopes were binned at 3x3 pixels. This binning factor could be further increased to 6x6 or 8x8 to greatly reduce CCD readout time. One disadvantage of this approach is an increased potential for background field star contamination given the larger collection area per pixel. Another potential adjustment is reading out only the center of the CCD, decreasing the readout time. This approach will place more constraints on pointing accuracy given the reduced field of view, motivating time-varying rate tracking. When applied in tandem, increased binning and reducing the CCD readout area promise to significantly reduce the sampling periods. These improvements will be implemented in future observation campaigns.

5. CONCLUSION

In all, this paper presented analysis of several retired geosynchronous satellite light curves. The preliminary rotation states of the satellites ranged from uniform to tumbling motion. At least one satellite, GOES 8, appears to be continuously evolving into a more complex tumbling rotation state. GOES 10 may be evolving as well, but more observations are needed to confirm this. On the other hand, the tumbling rotation state of GOES 9 does appear to have changed between 2014 and 2016. This is intriguing given that it is nearly identical to GOES 8 in construction and was retired three years later. If GOES 9 has in fact reached a stable tumbling equilibrium, that would suggest multiple evolutionary paths for retired geosynchronous satellites, not all of which are cyclical or terminate in uniform rotation about the maximum moment of inertia. Furthermore, tumbling motion is not a minimum energy state, suggesting that the YORP effect and other environmental torques are acting on GOES 9 to maintain a constant tumbling state. To further investigate the hypothesis of Albuja et al. that some retired geosynchronous satellites undergo cyclic rotation state evolution, future work will include a detailed analysis of the 2015-2016 GOES 8 light curves to determine the rotation states corresponding to the observed rotation periods. This period assignment process will take advantage of GOES 8's known moments of inertia and shape. Hopefully this detailed analysis will reveal how the satellite's tumbling state is evolving. In addition, observations of a tumbling satellite such as GOES 8, GOES 9, or Inmarsat-2 F2 returning to uniform motion would be needed to confirm the cyclical hypothesis of Albuja et al. Therefore, observations of these and other retired geosynchronous satellites will continue to be gathered and analyzed to better understand their rotational motion.

ACKNOWLEDGMENTS

This work was supported by a NASA Space Technology Research Fellowship.

The authors would also like to thank William and Eileen Ryan for kindly sharing their GOES 8 observation data.

REFERENCES

1. Albuja A., Scheeres D., McMahon J., (2015). Evolution of angular velocity for defunct satellites as a result of YORP: An initial study, *Advances in Space Research*, **56**(2), 237–251
2. Albuja A., Scheeres D., Cognion R., Ryan W., Ryan E., The YORP Effect on the GOES 8 and GOES 10 Satellites: A Case Study, *Advances in Space Research*, (in review)
3. Cognion R., (2013). Large phase angle observations of GEO satellites, *Proceedings of SPIE Sensors and Systems for Space Applications VI*, **8739**
4. Cognion R., (2014). Rotation rates of inactive satellites near geosynchronous earth orbit, *Proceedings of the 2014 Advanced Maui Optical and Space Surveillance Technologies Conference*
5. Flohrer T., (2015) Classification of geosynchronous objects, European Space Operations Center, Issue 17
6. Flohrer T., (2016) Classification of geosynchronous objects, European Space Operations Center, Issue 18
7. Hall D., et al., (2006). AMOS Observations of NASA's IMAGE Satellite, *Proceedings of the Advanced Maui Optical and Space Surveillance Technologies Conference*
8. Kaasalainen M., (2001). Interpretation of lightcurves of precessing asteroids, *Astronomy & Astrophysics*, **376**(1), 302–309
9. Karavaev Y., Kopyatkevich R., Mishina M., et al., (2005). The dynamic properties of rotation and optical characteristics of space debris at geostationary orbit, *Advances in Astronautical Sciences*, **119**(4), 1457-1466
10. Mueller B., Samarasinha N., Belton M., (2002). The Diagnosis of Complex Rotation in the Lightcurve of 4179 Toutatis and Potential Applications to Other Asteroids and Bare Cometary Nuclei, *Icarus*, **158**(2), 305–311
11. Papushev P., Karavaev Y., Mishina M., (2009). Investigations of the evolution of optical characteristics and dynamics of proper rotation of uncontrolled geostationary artificial satellites, *Advances in Space Research*, **43**(9), 1416-1422
12. NOAA Photo Library: Graphic of GOES I-M, the present generation of GOES-NEXT satellites, http://www.photolib.noaa.gov/htmls/spac0256.htm, Retrieved Apr. 5, 2017
13. Pravec P., et al., (2005). Tumbling Asteroids, *Icarus*, **173**(1), 108–131
14. Ryan W., Ryan E., (2015). Photometric Studies of Rapidly Spinning Decommissioned GEO Satellites, *Proceedings of the 2015 Advanced Maui Optical and Space Surveillance Technologies Conference*
15. Samarasinha N., Mueller B., (2015). Component periods of non-principal-axis rotation and their manifestations in the lightcurves of asteroids and bare cometary nuclei, *Icarus*, **248**, 347–356